

An Efficient Source of Single Photons: A Single Quantum Dot in a Micropost Microcavity

Matthew Pelton,^{*} Charles Santori, Jelena Vučković, Bingyang Zhang,[†]

Glenn S. Solomon,[‡] Jocelyn Plant, and Yoshihisa Yamamoto[†]

*Quantum Entanglement Project, ICORP, JST, E. L. Ginzton Laboratory,
Stanford University, Stanford, California, 94305 U.S.A.*

(Dated: October 22, 2018)

We have demonstrated efficient production of triggered single photons by coupling a single semiconductor quantum dot to a three-dimensionally confined optical mode in a micropost microcavity. The efficiency of emitting single photons into a single-mode travelling wave is approximately 38%, which is nearly two orders of magnitude higher than for a quantum dot in bulk semiconductor material. At the same time, the probability of having more than one photon in a given pulse is reduced by a factor of seven as compared to light with Poissonian photon statistics.

PACS numbers: 42.50.Ct, 42.50.Dv, 78.67.Hc, 85.60.Jb

The photon statistics of a light source can be described by the second-order autocorrelation function, defined as follows: $g^{(2)}(\tau) = \langle \hat{a}^\dagger(t) \hat{a}^\dagger(t + \tau) \hat{a}(t + \tau) \hat{a}(t) \rangle / \langle \hat{a}^\dagger \hat{a} \rangle^2$, where $\hat{a}^\dagger(t)$ and $\hat{a}(t)$ are the photon creation and annihilation operators, respectively, at time t . A pulsed source will have a correlation function consisting of a series of peaks separated by the repetition period T . The area $g_o^{(2)}$ of the peak around $\tau = 0$, normalized by T , gives an upper bound on the probability that two or more photons are present in the same pulse: $P(n \geq 2) \leq (1/2) \langle \hat{n} \rangle^2 g_o^{(2)}$, where $\langle \hat{n} \rangle$ is the mean photon number per pulse [1]. A source where $g_o^{(2)} < 1$ has a reduced multi-photon probability as compared to coherent light with Poissonian photon statistics. If $g_o^{(2)}$ is sufficiently close to zero, we can speak of a *single-photon source*.

Such a source has been demonstrated using the controlled excitation of single molecules [2, 3] and single nitrogen-vacancy centers in diamond nanocrystals [4], and using the controlled injection of carriers into a mesoscopic quantum well [5]. Pulsed excitation of semiconductor quantum dots (QD's) can also be used for single-photon production [1, 6]. The energy of the photon emitted due to electron-hole recombination in a dot depends on the total charge configuration of the dot [7]. If we excite a QD with a laser pulse, then, the electron-hole pairs that are created will each recombine to emit a photon with a unique wavelength. A single emitted photon can subsequently be isolated by spectral filtering [8].

QD's offer several advantages as sources for single photons. They have high oscillator strengths and narrow spectral linewidths, and do not suffer from photobleaching or shelving. The materials used to make QD's are compatible with mature semiconductor technologies, allowing them to be further developed and integrated with other components. A significant drawback, though, is that very few of the photons emitted by a QD escape from the high-refractive-index semiconductor containing the dot into useful directions. This can be remedied by

placing the dot in a microscopic optical cavity, increasing the spontaneous emission rate by a quantity known as the Purcell factor. The fraction β of the emitted photons which are captured by the cavity mode then depends on the enhanced emission rate γ and the emission rate γ_o in the absence of a cavity: $\beta = 1 - (\gamma_o - \gamma_c)/\gamma$, where γ_c/γ_o is the fraction of radiation that would be coupled into the cavity mode in the limit of zero photon storage time.

In order to have an efficient source of single photons, it is necessary that a large fraction of the light escapes from the confined cavity mode into a single travelling-wave mode. This extraction efficiency can be determined by comparing the quality factor Q of the mode in a real cavity to the quality factor Q_o for an ideal cavity without unwanted losses: $\eta_{\text{extract}} = Q/Q_o$. The mean photon number per pulse that can be observed will also depend on the total collection and detection efficiency of the experimental apparatus. Since this is not intrinsic to the single-photon source, we will concentrate on the external quantum efficiency η of the device, independent of the measurement equipment.

Several semiconductor microcavities have been investigated for the enhancement of spontaneous emission from QD's, including whispering-gallery modes in microdisks [9] and defect modes in two-dimensional photonic crystals [10, 11]. More practical for light extraction are microscopic posts etched out of distributed-Bragg reflector (DBR) microcavities [12, 13]. Light escaping from the fundamental mode of a micropost microcavity is well approximated by a Gaussian beam, and can thus be efficiently coupled into optical fibers, detectors, or other downstream optical components.

We used molecular-beam epitaxy to grow planar DBR microcavities containing self-assembled InAs QD's. The DBR mirrors consist of alternating quarter-wavelength-thick layers of GaAs and AlAs, separated by a one-wavelength-thick spacer layer of GaAs. The reflectivity of the bottom DBR was designed to be significantly higher

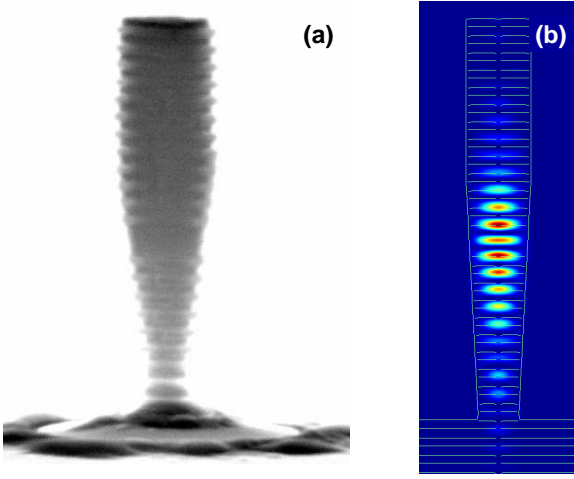


FIG. 1: (a) Scanning-electron microscope (SEM) image of a micropost microcavity with a top diameter of $0.6 \mu\text{m}$ and a height of $4.2 \mu\text{m}$. (b) Color-scale representation of the amplitude of the electric field for the fundamental mode of the micropost microcavity, as calculated by the finite-difference time-domain method. The profile of the modelled post matches the profile of the real posts, as measured from SEM images.

than that of the top DBR, so that almost all of the light in the cavity escapes upwards rather than downwards. The QD's were grown at the center of the spacer layer. They are islands of InAs formed by a strain-induced self-assembly process [14]. We grew islands with a low areal density by using a high substrate temperature and by stopping InAs deposition shortly after island formation.

Following the growth, we etched microposts out of the sample. A bilayer resist was exposed using an electron beam and was subsequently used to lift off a thick nickel mask. The sample was then etched using a low-pressure electron-cyclotron-resonance plasma of chlorine and boron trichloride in a background of argon. We divided the etch into three stages; in each subsequent stage, we decreased the flow rate of chlorine and decreased the process pressure. The sample was cooled to an initial temperature of about 3°C before the etch was started. Fig. 1(a) shows a scanning-electron microscope image of a typical etched micropost. Light in the post is confined vertically by the DBR's and laterally by total internal reflection.

For optical measurements, pulsed laser light with a photon energy larger than the GaAs bandgap was directed towards the micropost. The sample was held in a liquid-helium cryostat at a temperature of approximately 5 K, so that the created carriers were rapidly trapped by the QD and quickly relaxed to the lowest-energy confined states. Optical emission was collected by a lens in front of the cryostat and was filtered spectrally and spatially to eliminate scattered pump light. The emit-

ted light could be sent to a spectrometer (with a spectral resolution of 0.05 nm) or to a streak camera (with a temporal resolution of 25 ps), for measurement of intensity as a function of time and of wavelength. Alternatively, it could be directed towards a Hanbury Brown and Twiss-type (HBT) apparatus, which incorporated spectral filtering, in order to record a histogram of time intervals between photons. In the limit of low total collection and detection efficiency, this histogram approximates the photon correlation function $g^{(2)}(\tau)$. More detail on the experimental methods can be found in Ref. [15].

We used selected a particular post, with a top diameter of $0.6 \mu\text{m}$, which exhibited a single-QD photoluminescence line at a wavelength of 855 nm , spectrally well removed from the wetting-layer emission. A visibility of $33.1 \pm 1.8 \%$ was measured in a linear polarization basis for this emission line, while very low visibility was measured in a circular basis. We therefore modelled light from the QD as consisting of a linearly polarized part together with an unpolarized part in determining the fraction of QD emission lost at the polarizers in our HBT setup.

Single-photon generation was confirmed using the HBT apparatus. A measured histogram is shown in Fig. 2(a). The central peak is nearly absent, reflecting strong suppression of the multi-photon probability. Each peak in the photon correlation data can be described by a two-sided exponential, with a decay constant given by the spontaneous decay time and the instrument response time. The recombination time was measured using the streak camera to be $4.4 \pm 1.2 \text{ ns}$. (Details on lifetime measurements are given in Ref. [16].) The time resolution of the HBT apparatus was calibrated by measuring correlation functions for attenuated laser light scattered off the micropost. The width of the measured peaks was $473 \pm 29 \text{ ps}$, mostly limited by electronic jitter in our photon counters.

A fit using the measured time constants is also shown in Fig. 2(a); the only two adjustable parameters are the area of the central peak and the area of all the other peaks. The ratio of these areas, equal to $g_o^{(2)}$, is shown for various pump powers in Fig. 2(b). The probability of multi-photon pulses increases with pump power, suggesting that other states, apart from the desired QD emission, are contributing a background of unregulated photons.

The overall detection efficiency after the initial collection lens was determined by scattering attenuated laser light, tuned to the QD emission wavelength, off the micropost of interest. The total photon count rate at the detectors was compared to the optical power measured immediately after the collection lens using a calibrated power meter. Including light lost at the polarizers, the detection efficiency was determined to be $3.02 \pm 0.16 \%$.

The fraction of light captured by the initial lens, on the other hand, was estimated to be 22% using Gaussian-

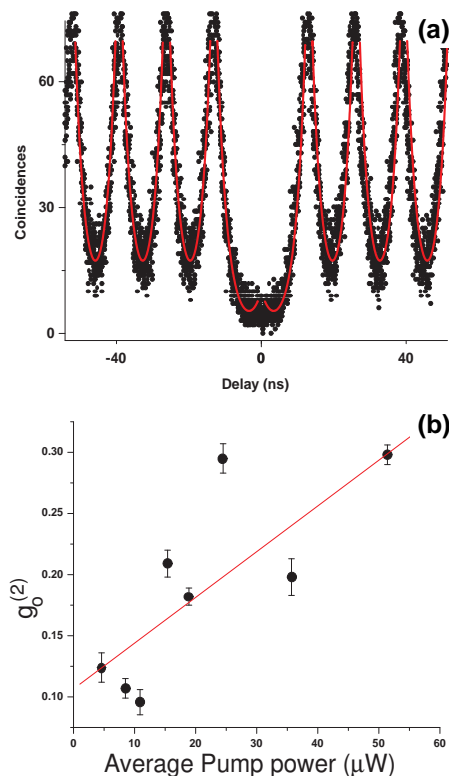


FIG. 2: (a) Measured autocorrelation for photons from a single quantum dot in a micropost microcavity, for an incident pump power of $10.9 \mu\text{W}$ and an integration time of 300 s (points), and corresponding fit (line). Due to the relatively low emission rate from the QD, adjacent peaks overlap. (b) Area of the central autocorrelation peak relative to the area of the side peaks as a function of pump power (points). The solid line is a guide to the eye.

beam optics, with the beam waist in the post being approximated by the fundamental mode in an infinite cylindrical waveguide. This estimate was validated by calculations using the finite-difference time-domain (FDTD) method. The field distribution in the fundamental mode was calculated as described in Ref. [17]; Fig. 1(b) shows the result. The far-field radiation pattern was then estimated by Fourier-transforming the calculated near field [18]. The result shows a nearly Gaussian profile, with a divergence that agrees well with that given by Gaussian-beam optics.

In order to determine the device efficiency, the total photon count rate was normalized by the laser repetition rate and then divided by the collection and detection efficiency, giving the mean photon number per pulse $\langle \hat{n} \rangle$. We then assumed that the light emitted from the source consists of a statistical mixture of perfectly regulated single photons, together with a small background of photons with Poissonian statistics. The coupling of this state into the travelling-wave mode leaving the top of the micropost was modelled as an attenuation by a factor equal to

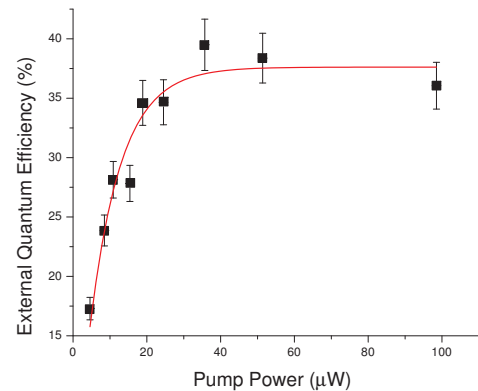


FIG. 3: External quantum efficiency of a single-photon source consisting of a single quantum dot in a micropost microcavity as a function of pump power (points), together with a saturation fit (line).

the efficiency η , giving $\eta = \langle \hat{n} \rangle (1 - g_o^{(2)})^{1/2}$.

Fig. 3 shows efficiencies determined in this way. The efficiency saturates at higher powers, when more than one electron-hole pair is captured by the dot for each pump pulse. The solid line is a fit according to the saturation equation $\eta = \eta_{\text{max}}(1 - e^{-P/P_{\text{sat}}})$, where P_{sat} is the saturation pump power and the saturated efficiency η_{max} is equal to $37.6 \pm 1.1\%$. This external quantum efficiency is approximately two orders of magnitude higher than that for a QD in bulk GaAs. We believe that this is also the highest efficiency yet reported for a single-photon source. We note that, in determining this efficiency, we have not considered the polarization states of the emitted photons. We also note that the efficiency drops to approximately 8% if we include losses at the initial collection lens; however, this could be improved simply by using a lens with a larger numerical aperture.

The measured efficiency should be equal to the product of the coupling coefficient β and the light extraction efficiency η_{extract} . Under high pump power, the discrete QD transition is accompanied by a broadband background, filtered by the cavity resonance; a Lorentzian fit to the filtered luminescence gives $Q = 628 \pm 69$. A similar measurement on an unetched portion of the planar microcavity gives $Q_o = 1718 \pm 13$, resulting in $\eta_{\text{extract}} = 36.6 \pm 4.0\%$. The coupling coefficient, on the other hand, was determined by measuring the recombination rates for other QD's on the same sample that are out of resonance with the cavity mode. The off-resonant lifetimes are expected to be nearly identical to the lifetimes of QD's in the absence of a microcavity, due to the high density of leaky modes in our micropost microcavities [19]. Since the unmodified lifetimes are too long to measure using our streak camera, we measured the autocorrelation of photons from these dots using the HBT apparatus, and fitted the peak widths to obtain a

recombination time of 25.4 ± 1.4 ns. This represents a Purcell factor of 5.8 ± 1.6 , corresponding to a coupling coefficient $\beta = 83 \pm 23\%$. We note that the unmodified lifetimes are unusually long for self-assembled InAs / GaAs QD's. However, the demonstrated improvement of collection efficiency using the Purcell effect is independent of the exact nature of the dots, and should apply equally to QD's with shorter lifetimes.

Combining the measured β and η_{extract} results in an expected external quantum efficiency of $30 \pm 9\%$. This agrees, within the error, with the efficiency that we determined at saturation.

Both β and η_{extract} are limited by the quality factor of the microcavity mode. FDTD simulations predict $Q = 657$ for our micropost, in good agreement with the experimental value. Since the calculations do not include non-idealities such as surface roughness, the difference between Q for the micropost and Q_o for the planar microcavity can be attributed to the post geometry. Improving Q requires more vertical post sidewalls, which should be achievable using different etching techniques, such as chemically assisted ion-beam etching. Optimization of the microcavity design can increase the quality factor yet further, allowing for coupling efficiencies approaching 100% [20].

To summarize, we have demonstrated efficient generation of single photons using a single quantum dot in a micropost microcavity. The emission rate from the dot was enhanced by a factor of 5.8, so that 83% of the emitted light was coupled into a single cavity mode. The majority of this light escaped into a single-mode, Gaussian-like travelling wave, resulting in an external quantum efficiency of approximately 38%. This high efficiency is achieved at the same time that the probability of having more than one photon in a given pulse is reduced by a factor of seven as compared to Poissonian light. We note that single-photon generation using a single QD in a micropost microcavity has recently been reported by other researchers [21], but no explicit treatment of device efficiency has been provided.

An efficient source of single photons will be useful for quantum key distribution [22]. Using existing single-photon sources would result in a limited secure-key transmission rate over reasonable distances, due to the accumulated effects of source inefficiency, channel loss, and compression during error correction and privacy amplification. Our demonstrated improvement in source efficiency would allow for transmission through approximately 20 dB of additional channel loss. Our single-photon source may also eventually be useful for linear-optical quantum computation, providing the very high efficiencies required, while emitting indistinguishable photons capable of exhibiting the necessary fourth-order interference [23].

We would like to thank E. Waks and A. Scherer for helpful discussions. Financial assistance for M.P. and

C.S. was provided by Stanford University. Financial assistance for C.S. was also provided by the National Science Foundation. Financial assistance for G.S.S. was provided by the Army Research Office.

* Current Address: Laboratory of Quantum Optics and Quantum Electronics, Department of Microelectronics and Information Technology, Royal Institute of Technology (KTH), Electrum 229, SE-164 40 Kista, Sweden; Electronic address: pelton@imit.kth.se

† Also at NTT Basic Research Laboratories, Atsugishi, Kanagawa, Japan

‡ Also at Solid-State Photonics Laboratory, Stanford University, Stanford, California, 94305 U.S.A.

- [1] C. Santori, M. Pelton, G. S. Solomon, Y. Dale, and Y. Yamamoto, Phys. Rev. Lett. **86**, 1502 (2001).
- [2] C. Brunel, B. Lounis, P. Tamarat, and M. Orrit, Phys. Rev. Lett. **83**, 2722 (1999).
- [3] B. Lounis and W. E. Moerner, Nature **407**, 491 (2000).
- [4] A. Beveratos, S. Kühn, R. Brouri, J.-P. Poizat, and P. Grangier, Eur. Phys. J. D **18**, 191 (2002).
- [5] J. Kim, O. Benson, H. Kan, and Y. Yamamoto, Nature **397**, 500 (1999).
- [6] P. Michler, A. Kiraz, C. Becher, W. V. Schoenfeld, P. M. Petroff, L. Zhang, E. Hu, and A. Imamoglu, Science **290**, 2282 (2000).
- [7] L. Landin, M. S. Miller, M.-E. Pistol, C. E. Pryor, and L. Samuelson, Science **280**, 262 (1998).
- [8] J.-M. Gérard and B. Gayral, J. Lightwave Technol. **17**, 2089 (1999).
- [9] B. Gayral, J. M. Gérard, A. Lemaître, C. Dupuis, L. Manin, and J. L. Pelouard, Appl. Phys. Lett. **75**, 1908 (1999).
- [10] C. Reese, C. Becher, A. Imamoglu, E. Hu, B. D. Gerardot, and P. M. Petroff, Appl. Phys. Lett. **78**, 2279 (2001).
- [11] T. Yoshie, A. Scherer, H. Chen, D. Huffaker, and D. Deppe, Appl. Phys. Lett. **79**, 114 (2001).
- [12] J. M. Gérard, B. Sermage, B. Gayral, B. Legrand, E. Costard, and V. Thierry-Mieg, Phys. Rev. Lett. **81**, 1110 (1998).
- [13] G. S. Solomon, M. Pelton, and Y. Yamamoto, Phys. Rev. Lett. **86**, 3903 (2001).
- [14] D. Bimberg, M. Grundmann, and N. N. Ledentsov, *Quantum Dot Heterostructures* (John Wiley & Sons, Chichester, 1999).
- [15] C. Santori, D. Fattal, M. Pelton, G. S. Solomon, and Y. Yamamoto, Phys. Rev. B **66**, 045308 (2002).
- [16] C. Santori, G. S. Solomon, M. Pelton, and Y. Yamamoto, Phys. Rev. B **65**, 073310 (2002).
- [17] M. Pelton, J. Vučković, G. S. Solomon, A. Scherer, and Y. Yamamoto, IEEE J. Quantum Electron. **38**, 170 (2002).
- [18] J. Vučković, M. Lončar, H. Mabuchi, and A. Scherer, IEEE J. Quantum Electron. **38**, 850 (2002).
- [19] M. Bayer, T. L. Reinecke, F. Weidner, A. Larinov, A. McDonald, and A. Forchel, Phys. Rev. Lett. **86**, 3168 (2001).
- [20] J. Vučković, M. Pelton, A. Scherer, and Y. Yamamoto, to appear in Phys. Rev. A.
- [21] E. Moreau, I. Robert, J. M. Gérard, I. Abram, L. Manin, and V. Thierry-Mieg, Appl. Phys. Lett. **79**, 2865 (2001).

- [22] N. Lütkenhaus, Phys. Rev. A **61**, 052304 (2000).
- [23] E. Knill, R. Laflamme, and G. J. Milburn, Nature **409**, 46 (2001).